# An Improved Harris-Affine Invariant Interest Point Detector

KARINA PEREZ-DANIEL, ENRIQUE ESCAMILLA,
MARIKO NAKANO, HECTOR PEREZ-MEANA
Mechanical and Electrical Engineering School
Instituto Politecnico Nacional
Av. Santa Ana 1000, Col. San Francisco Culhuacan, 04430 Mexico D.F.
MEXICO
hmperezm@ipn.mx http://www.posgrados.esimecu.ipn.mx

*Abstract:* - Interest point detection is essential process for many computer vision applications, which must provide invariant points to several image variations, such as, rotation, zoom, blur, illumination variation and change of viewpoints. Harris-Affine detector is considered as one of the most effective interest point detectors, although it still presents vulnerability to some image. This paper proposes an improved Harris-affine interest point detector based on two-dimensional weight Atomic functions to improve the repeatability and stability of detected points of Harris-Affine detector, in which the Gaussian kernel is replaced by the $up(x)$ Atomic Function. Evaluation results show that the new image interest point detector, called Atomic Harris-Affine detector, improves the repeatability in about 40% compared with the conventional Harris-Affine detector, under several conditions such as blurring, illumination changes, change of viewpoint, as well as other geometrical and affine transformations.

*Key-Words:* - interest points detector; Atomic function; Harris-Affine detector; repeatability; convergence rate

## 1 Introduction

Interest point detection is a core problem of many computer vision applications, such as image recognition, learning visual categories, 3D reconstruction, image mosaicing, image retrieval [1-4]. Interest points make possible estimating a set of local features that are invariant to a variety of viewing conditions such as blur, zoom, rotation, affine variations, illumination changes, partial occlusion, etc. This set of local features is essential for the above mentioned applications, because they can define, uniquely, the spatial location, orientation and scale of each object in a scene. Therefore, several interest point detectors have been proposed during the last several years, which are Harris [5], Harris-Laplace [6], Harris-Affine [7], Susan [8], LoG [9], etc. However, almost all of them still present several difficulties in achieving invariance under several viewing conditions.

An efficient interest point detector must satisfy, besides geometrical invariance, three other main properties. First, interest point detector should be robust to the variations of its capture condition, such as noise, blurring or illumination changes. Second, interest points should clearly stand out against its neighborhood, being as distinctive as possible. And third, high percentage of interest points detected from two images of the same object, taken under different viewing conditions should be detected in both images, i.e. high rate repeatability [10]. These properties are quite general for almost all applications; though depending on the application task, several properties can be more relevant than others. Until now, different problems of the interest point detection have been analyzed and reviewed by Moravec [11], Harris and Stephens [5], Shi and Tomasi [12], Beaudet [13], Mokhtarian and Suomela [13], and some improvements presented in [6, 7] and [15, 16].

Most of the current local invariant interest point detectors are based on the classical interest point detectors, such as Harris and Hessian detectors, that are a fundamental part of several modern interest point detectors. Robustness to rotation, illumination variation and noise contamination are the principal advantages of Harris-based detector, which can be considered as one of the most reliable interest point detectors due to its accuracy shown in performance evaluations reported in [17-20], and in several applications reported in [21-23] where Harris or Harris-based detector has been successfully used. However, the interest points detected by Harris-based detector [5] are not invariant in scaling variation and drastic affine deformations. Therefore this detector was improved to be invariant to scale and affine transformations [7]. Recently several approaches to improve the Harris-based interest point detector have been proposed, for example in

[24] a non-parameter Harris-Affine detector is reviewed. Likewise Sipiran [25] proposed a 3D detection based on Harris detector, as well as Gevrekci and Kadir [26] present a method which improves the repeatability rate of Harris detector under illumination variations. However, almost all related works do not heed about the weak frequency response of the Gaussian kernel used in Harris-based detector. L. Zhang and D. Zhang [27] proposed a bilateral weighting function is used instead of Gaussian Function; however this algorithm was only evaluated using synthetic images.

Recently Atomic functions [28] are employed successfully to improve the performance in several signal and image processing applications requiring some kind of weighting operations such as pattern recognition [29], optical flow estimation [30]. In [31] we probe that the interest point detection can be improved if the Gaussian function is replaced with an atomic function in the conventional Harris detector, especially for blurred or smoothed images and images captured by different viewpoints. Considering that Harris-Affine is based on affine normalization around multi-scale Harris points, which implies several filtering operations based on Gaussian kernel, therefore applying Atomic Function instead of Gaussian function, the detection accuracy can be expected to be improved notably.

This paper proposes an improved *Harris-Affine* detector interest point which a Gaussian function is replaced by an Atomic function to improve the repeatability rate of interest points under several imagining conditions, such as illumination level, blurring level, viewpoints and any affine transform including rotation, scaling and shearing. The proposed detector provides not only a higher accuracy of interest point detection, but also a better convergence property than that of the conventional Harris-Affine detector.

The rest of the paper is organized as follows, Section 2 gives a description of Multi-scale Harris, Harris-Laplace and Harris-Affine detector, Section 3 provides a description of the proposed interest point detector. Section 4 shows a performance of the proposed detector comparing with the conventional Harris-Affine detector and finally Section 5 presents the conclusion of this work.

# 2 Scale and Affine invariant Interest Point Detectors

Harris Detector [5] is one of the most popular corner-based detectors. Its strong invariance to rotation, noise contamination and illumination variations is the main reasons for this popularity. This detector has been extended giving as a result several other approaches such as Harris-Laplace [6] and Harris-Affine [6, 7, 32] which are respectively scale and affine invariant detectors. All those versions employ the second moment matrix to detect interest points in an image, which are used to recognize, classify and detect objects [33] among many other applications.

## 2.1 Harris Detector

Harris detector [5] is one of the interest points detector most used nowadays and recently has been shown an important relation with the computational visual attention model of visual perception [34]. Harris detector improved the approach proposed by Moravec [11] by performing an analytical expansion of the average intensity variance, wherein a "corner'" corresponds to a region of an image $I$ with locally maximized directional derivatives, within a neighborhood, in any $I_x$ and $I_y$ direction. The cornerness of Harris function is given by

$$cornerness = \det M - k(\text{trace}\, M)^2 \tag{1}$$

where $M$ is given by

$$M = \sum_{x,y} w(x,y) * \begin{bmatrix} {I_x}^2 & I_x I_y \\ I_x I_y & {I_y}^2 \end{bmatrix} \tag{2}$$

The term $w(x,y)$ represents the Gaussian kernel and $k$ is an arbitrary constant (usually determined between $0.02 < k < 0.06$) used to reduce the effect of a strong contour.

In order to achieve the *corner points* a threshold $th$ is established for the *cornerness* value. It is worth noting that the parameters $k$ and $th$ must be manually set to avoid false corner points. Then, the point *(x*,y) is considered as a *corner point* if $cornerness > th$. From the Eq. (2) the Eigenvalues $\lambda_1$ and $\lambda_2$ of $M$ matrix in Eq. (2) are yielded, which are essential to determine the value of the *cornerness*, as shown in Eq. (3).

$$\begin{aligned} \det M &= \lambda_1 * \lambda_2 \\ \text{trace}\, M &= \lambda_1 + \lambda_2 \end{aligned} \tag{3}$$

Hence using Harris detector three kinds of regions can be detected, i.e., if $\lambda_1$ and $\lambda_2$ are small, it

means a *flat* region. Moreover, if $\lambda_1>\lambda_2$ or $\lambda_1<\lambda_2$ it is referred to an *edge* region. A *corner* is detected when the eigenvalues $\lambda_1$ and $\lambda_2$ are larger in all directions.

## 2.2. Harris-Affine Detector

The scale & affine invariant version of Harris detector was introduced in [6], where the Harris-Laplace detector was extended to Harris-Affine detector to deal with any affine transformations, starting from the premise of the scale-space or multi-scale Harris Detector.

### 2.2.1. Multi-Scale Harris Detector

The Multi-scale Harris detector handles local image structures at different scales, when the scale factor increases the fine structures vanish while the coarser structures emerge. Multi-scale stage arises by modifying the second moment matrix $M$ to its *scale-space* version [40], resulting the following matrix $\mu$

$$\mu(x,y,\sigma_I,\sigma_D) = \sigma_D{}^2 w(\sigma_I) * \begin{bmatrix} L_x{}^2(x,y,\sigma_D) & L_xL_y(x,y,\sigma_D) \\ L_xL_y(x,y,\sigma_D) & L_y{}^2(x,y,\sigma_D) \end{bmatrix} \quad (4)$$

where $L_i(x,y,\sigma_D)$ is the first partial derivative along the $i$ direction on the image $I(x,y)$ at the scale $\sigma_D$, given by

$$L_i(x,y,\sigma_D) = w(x,y,\sigma_D) * I(x,y), \quad (5)$$

where "*" denotes the convolution operator, $w(\sigma_I)$ is the scale-space version of the filtering kernel, and $\sigma_I$ is the integration scale and $\sigma_D$ is the differentiation scale. The 2x2 matrix of Eq. (4) describes the gradient distribution in a local neighborhood. Thus the local derivatives $L_i(x,y,\sigma_I)$ are computed using the Gaussian kernels determined by the local scale $\sigma_D$ which are then averaged using the Gaussian kernel of size $\sigma_I$ around the neighborhood of the point $(x,y)$. In this way the eigenvalues of this matrix indicate characteristics of the point in its neighborhood that is significant change in the orthogonal direction i.e. corners. Hence, taking in account the multi-scale concept, the Harris cornerness is given by

$$cornerness = \det\left(\mu(x,y,\sigma_I,\sigma_D)\right) - k\,\mathrm{trace}^2\mu(x,y,\sigma_I,\sigma_D) \quad (6)$$

The local maxima of cornerness determine the location of scale invariant interest points.

### 2.2.2. Harris-Laplace Detector

Harris-Laplace detector [6] uses the scale adapted Harris function shown in the Eq. (4) to detect the interest points at different scales, according to the next equation

$$\sigma_n = \xi^n \sigma_0 \quad (7)$$

where $\sigma_n$ represents a pre-selected set of scales and $\xi$ is the scale factor between successive levels (experimentally set to 1.4). Thus Eq. (4) is computed with $\sigma_I=\sigma_n$ and $\sigma_D=s\sigma_n$, where $s$ is a constant factor (generally set to 0.7).

Harris-Laplace detector selects the points for which the Laplacian of the Gaussian function [35] (see Equation (8)) attains a maximum over scale in an iterative way. In this manner Harris-Laplace simultaneously detects the location and the scale of interest points.

$$|LOG(x,y,\sigma_n)| = \sigma_n{}^2 \left| L_{xx}(x,y,\sigma_n) + L_{yy}(x,y,\sigma_n) \right| \quad (8)$$

Thus, Harris-Laplace detector finds the best location at this scale according to (6) and the most suitable scale between the finer and the coarser level according to (8).

### 2.2.3. Harris-Affine Detector

The basic idea introduced by Harris-Affine detector is to select the characteristic scale and the characteristic elliptic shape iteratively using the second moment matrix, given by [32]

$$\mu(x,y,\Sigma_I,\Sigma_D) = \det(\Sigma_D) w(x,y,\Sigma_I) * \begin{bmatrix} L_x{}^2(x,y,\Sigma_D) & L_xL_y(x,y,\Sigma_D) \\ L_xL_y(x,y,\sigma_D) & L_y{}^2(x,y,\Sigma_D) \end{bmatrix} \quad (9)$$

Equation (9) is used to estimate the anisotropic shape of a neighborhood of the interest point. The integration and differentiation of the Gaussian kernels are determined by the covariance matrices $\Sigma_I$ and $\Sigma_D$, respectively, which differ in scale but not in shape. Note that this procedure involves a 2D convolution, which is computationally very expensive.

To reduce the computational cost and limit the search space, the eigenvalues of the second moment matrix are calculated according to (4). To obtain the

shape adaptation matrix, the eigenvalues obtained from (4) are used to measure the *affine* shape of the point neighborhood. In [7] it is supposed that a local *anisotropic* structure is a representation of an affine transformed *isotropic* one. For that reason, it is necessary to find the transformation that projects the anisotropic pattern to its isotropic related structure. This transformation is done by normalizing the shape adaptation matrix, such that the obtained isotropic structure must provide equal eigenvalues, in terms of the second moment matrix $\mu(x, y, \sigma_I, \sigma_D)$, which are used to measure the affine shape of the neighborhood of the point. Thus, the affine normalization of points $(x_R,y_R)$ and $(x_L,y_L)$ is given by the transformation shown in Eq. (10)

$$\begin{aligned}(x'_R, y'_R) &= (x_R, y_R)\mu_R^{1/2} \\ (x'_L, y'_L) &= (x_L, y_L)\mu_L^{1/2}\end{aligned} \tag{10}$$

Such that, the normalized regions are related by a simple rotation $(x_R,y_R)=R(x_R,y_R)= R(x'_R,y'_R)$ and the affine deformation can be determined by a rotation factor $R$, according to Baumberg [37], as shown in Fig, 1.

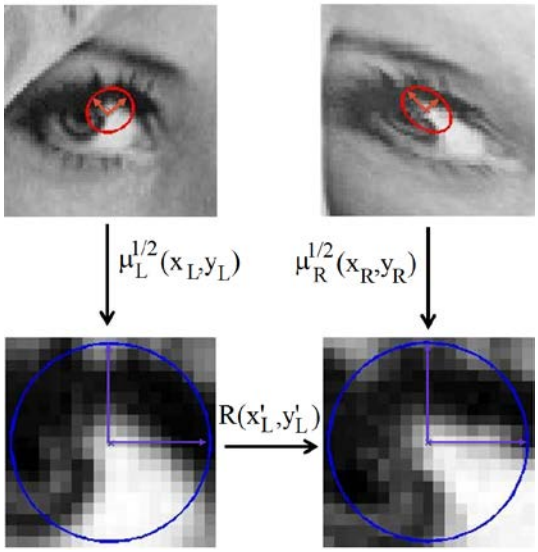


Fig.1. Isotropic neighborhoods related by image rotation

The local isotropy of the transformed region can be measured by the similarity of the eigenvalues $\lambda_{min}(\mu)$ and $\lambda_{max}(\mu)$ of the second moment matrix $\mu(x, y, \sigma_I, \sigma_D)$, as shown below

$$Q = \frac{\lambda_{\min}(\mu)}{\lambda_{\max}(\mu)} \tag{11}$$

where $Q$ is the normalized measure of the isotropy and varies in the range $0 < Q \leq 1$, being $Q = 1$ a perfect isotropic structure.

On the other hand the shape adaptation matrix is calculated by transforming the image using the U-transformation shown in (12) applying a uniform kernel instead of applying the elliptical Affine Gaussian kernel, i. e., a local window $w$ (decomposed into two 1D convolutions) is centered at interest point $(x, y)$ and it is transformed by (12) as shown in [6]

$$U^{(k-1)} = \left(\mu^{-1/2}\right)^{(k-1)} \ldots \left(\mu^{-1/2}\right)^{(1)} . U^{(0)} \tag{12}$$

For any $k$ iterations, the integration and differentiation scale determine the second moment matrix $\mu$. To calculate the maximum of the Harris cornerness around the point $(x_w,y_w)$ in the affine normalized window $W$, it is necessary to correct the initial point translating it using the displacement vector and inverse transforming the resulting point to get the image in the original domain [6].

$$\begin{aligned}\left(x^{(k)}, y^{(k)}\right) = \left(x^{(k-1)}, y^{(k-1)}\right) + U^{(k-1)} \cdot \\ \left(\left(x_w^{(k)}, y_w^{(k)}\right) - \left(x_w^{(k-1)}, y_w^{(k-1)}\right)\right)\end{aligned} \tag{13}$$

These two last steps are iteratively done until the second moment matrix shows isotropic image regions, according to the convergence ratio as follows [6]

$$(1 - Q) < 0.05 \tag{14}$$

Thus, when (14) is true the value of $Q$ is sufficiently close to 1, which means a perfect isotropic structure, and then the second moment of the transformed region is sufficiently close to a pure rotation, by the other hand, divergence is used to discard features with eccentric deformations, according to the next Equation [6]

$$\frac{\lambda_{\min}(U)}{\lambda_{\max}(U)} < 6 \tag{15}$$

## 3 Proposed Interest Point Detector

Several interest point detectors invariant to scale and affine distortions have been developed during the last several years as shown in Section 2. Among them, the Harris-Affine [7] detector, which selects

image regions that have sufficient image-gradient energy in orthogonal directions, is one of the most widely used. However, this detector still presents vulnerability to some image variations due to non-efficient filter operation based on Gaussian kernel. To overcome this problem we proposed a Harris-Affine based detector in which Gaussian kernel is replaced by the $up(x)$ atomic function in each stage. This is because, generally Atomic functions have a compact support and recently it has been shown that if the Gaussian kernel is replaced by an Atomic function the accuracy of interest point detection can be improved [31].

The proposed Atomic Harris-Affine detector, where the Gaussian function is replaced by the atomic function $up(x, y)$, consists of the following steps:

a. Detect the initial regions at location $(x^{(0)},y^{)0)})$ and scale $\sigma_I^{(0)}$, using the Multiscale Harris detector [6], replacing the Gaussian function by *up(x,y)* as follows

$$\mu(x,y,\sigma_I,\sigma_D) = \sigma_D{}^2 up(\sigma_I) * \begin{bmatrix} L_x{}^2(x,y,\sigma_D) & L_xL_y(x,y,\sigma_D) \\ L_xL_y(x,y,\sigma_D) & L_y{}^2(x,y,\sigma_D) \end{bmatrix} \quad (16)$$

$$L_i(x,y,\sigma_D) = up(x,y,\sigma_D) * I(x,y) \quad (17)$$

b. Use the identity matrix *I* to initialize the shape adaptation matrix $U^{(0)}$.

c. For each $k$-th iteration an image region $W_{(x,y)}$ centered at the point $(x_w,y_w)$, i.e. at the coordinates of the *U*-transformed image must be normalized, such that

$$\left(x_w{}^{(k-1)}, y_w{}^{(k-1)}\right) = U^{(k-1)^{-1}}\left(x^{(k-1)}, y^{(k-1)}\right) \quad (18)$$

d. Select the integration scale $\sigma_I^{(k)}$ at the point $(x^{(k-1)},y^{(k-1)})$, which maximizes the absolute value of the Laplacian, as shown in (8). Note that the image derivatives are convolved with the $up(x, y)$ kernel.

e. Select the differentiation scale $\sigma_D^{(k)}=s\sigma_I^{(k)}$ for $s\in[0.5,K,0.75]$, so that the value of the isotropy ratio Q is maximum. Thus Q is calculated by computing the second moment matrix at the point $(x_w^{(k-1)},y_w^{(k-1)})$, from the image region W, i e., $\mu=\mu(x_w^{(k-1)},y_w^{(k-1)},\sigma_I^{(k)},\sigma_D^{(k)})$

f. From a maximum of the Harris cornerness (see (6)), detect the spatial location $(x_w^{(k)},y_w^{(k)})$ around $(x_w^{(k)},y_w^{(k)})$ and compute the localization of a region in the original image domain using (13).

g. Update the shape adaptation matrix to

$$U^{(k)} = \mu_i{}^{(k)} . U^{(k-1)} \quad (19)$$

$$\mu_i{}^{(k)} = \mu^{-1/2}\left(x_w{}^{(k-1)}, y_w{}^{(k-1)}, \sigma_I{}^{(k)}, \sigma_D{}^{(k)}\right) \quad (20)$$

h. Normalize $U^{(k)}$ such that $\lambda_{max}(U^{(k)})=1$.

i. Go to step b if the eigenvalues of the second moment matrix for the new point are not equal, according to the convergence criterion given by (14) or divergence according to (15).

It is worth noting that the operation number of proposed and conventional Harris-Affine is the same, because the values of $up(x, y)$ can be computed in advance and store in a table to be used when they are required.

Figure 2 illustrates the filter response of 2D-Gaussian and *2D-up(x,y)* kernel, operating in a derivative way to calculate the matrix $\mu$. The second and third columns show the filtered images in each stage. From this figure it follows that the resulting image filtered with *2D-up(x,y)* preserves more details compared with the corresponding Gaussian filtered image. Then, this characteristic of $up(x, y)$ function can be used to improve the Harris-Affine detector.

### 3.1 UP(x) Atomic function

The Atomic functions (AFs) were introduced in 1975 by Rvachev [36]. The most popular Atomic function is the termed $up(x)$ function which is given by (16). This function is generated by infinite convolutions of rectangular impulses

$$up(x) = \frac{1}{2\pi}\int_{-\infty}^{\infty} e^{jux} \prod_{k=1}^{\infty} \frac{\sin(u.2^{-k})}{u.2^{-k}} du, x \in [-1,1] \quad (21)$$

In general AFs provides better frequency response than the classical windows, reducing spectral leakage, which benefit many applications such as filtering, spectral analysis, detection accuracy, resolution and dynamic interval, etc. as exposed in [13]. Fig.3 shows the traditional 1D Gaussian kernel evaluated in the range [-1,1] and its spectrum, as well as the kernel and spectrum of *up(x)* function evaluated in the same range.

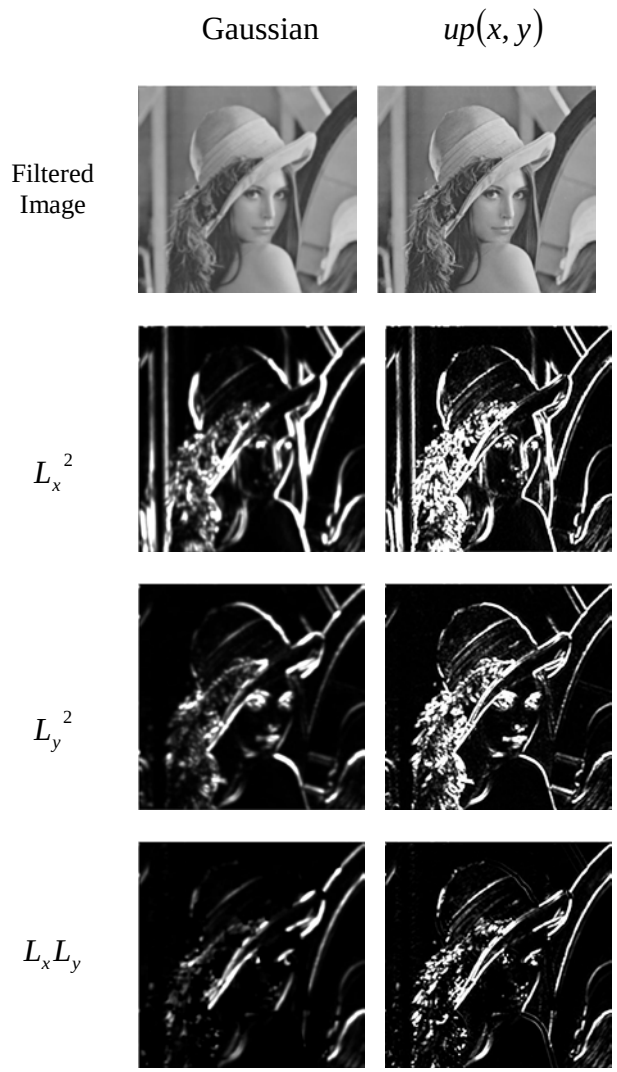


Fig. 2 Filtering performance of Gaussian and *up(x)* functions.

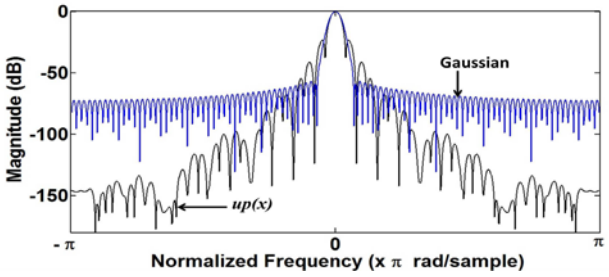


Fig. 3 Comparison of the Stop-band attenuation of *up(x)* Atomic Function and Gaussian Function

As shown in Fig. 3, AF functions allow to decrease the lateral side lobes and to increase the wide of the main lobe at the same time, improving in such way the performance of the interest point detector. The kernel shape of $up(x)$ allows to filter the image decreasing the information loss and smoothing in an effective way the image. The main advantages of the Atomic Functions lie on the spectral benefits [28].

Harris-Affine process involves several filtering operations using the Gaussian kernel; however this kernel introduces information loss as shown in Figures 2 and 3. This information loss causes a performance degradation of the conventional Harris-Affine detector; therefore the use of *up(x)* Atomic function instead of Gaussian function can be expected to improve the detection performance. To use the $up(x)$ function as 2D weighted function, firstly this function must be extended in 2D.

Fig. 4 Example of image sequences used for evaluation of the proposed detector.

## 4. Experimental Results

In this section, the performance of the proposed Atomic Harris-Affine is evaluated using several images stored in the database [37], as well as some other images. This database shows images which have been taken under several image conditions such as blurring, illumination changes, zooming and viewpoint changes, as shown in Fig. 4. To evaluate

ISBN: 978-1-61804-360-3

detection accuracy of interest points using both detectors: proposed and conventional one, the repeatability measure is used and also the detection accuracy improves the convergence property of scale and shape adaptation in both detectors. Both detectors are evaluated using the repeatability of detected interest points between two images with different image condition generated by a known homographic transformation. The repeatability gives a measure to determine the ratio between the numbers of corresponding regions centered by each interest point in a pair of images with different imaging condition which is given by

$$\text{Rep} = \frac{\#\ \text{of corresponding regions}}{\#\ \text{of detected regions}} \times 100 \qquad (22)$$

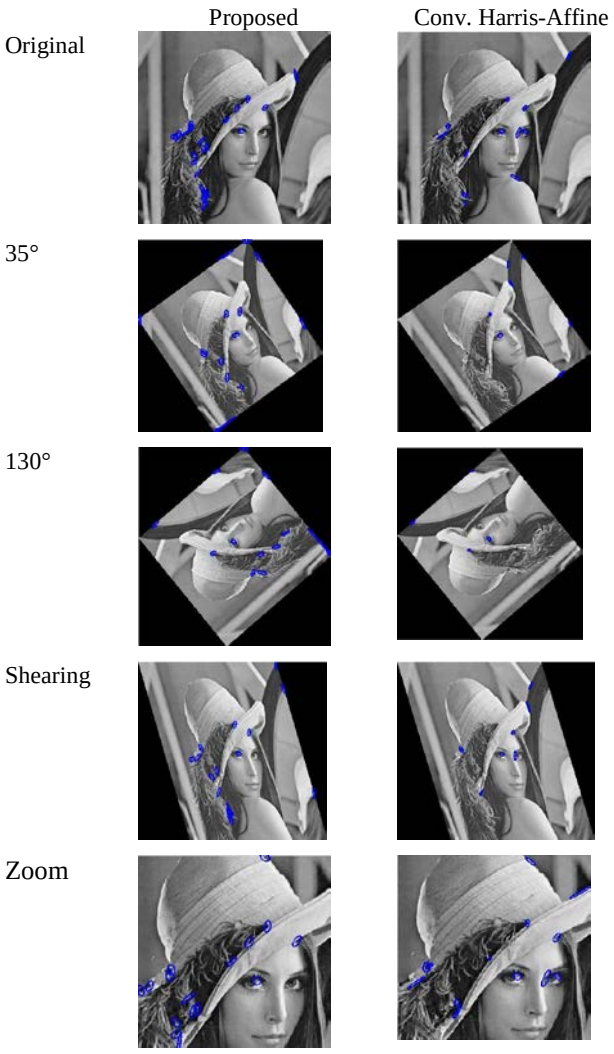


Fig. 5 Comparison of stability of the interest points detected by the proposed and conventional detectors when several geometrical distortions are applied

Figure 5 illustrates the performance comparison of the proposed Atomic Harris-Affine detector and the conventional one, showing detected interest points when several geometrical transforms are applied to "Lena" image. Again the interest points detected using proposed detector are more stable than these detected using the conventional Harris-Affine detector, especially when rotation and shearing are applied to the image. The repeatability rate given by (20) of proposed Atomic Harris-Affine and Harris-Affine detectors using images with several imaging condition shown in Fig. 4 are calculated, which are given in Fig. 6.

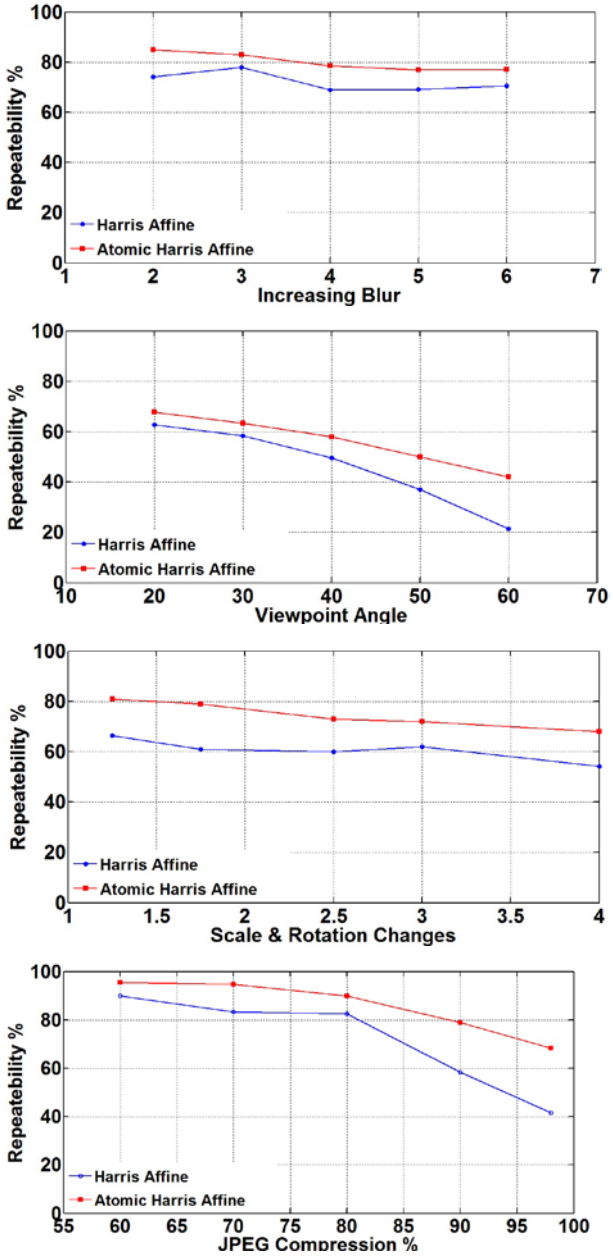


Fig. 6 Comparison of repeatability of interest points under several imagining condition.

Figure 6 shows the repeatability of interest points detected by proposed and conventional detectors under six different burring levels, it is notable the

improvement introduced by proposed approach providing 10%-30% better rates than the conventional one. It also shows the repeatability rates under different viewpoints. Again the proposed approach outperforms this rate by 5%-20% depending on viewpoint angles, compared with the conventional one. Fig. 6 provides also a comparison of the repeatability between both detectors under different scaling and rotation distortions. This type of distortion is commonly occurred, when a same scene is captured from different points including different distance between the object and viewpoint. Finally Fig. 6 shows this rate under lossy compression by JPEG algorithm with different compression rates. In both cases, the repeatability rate of the proposed detector is much better than that of the conventional one. In case of the illumination variation, improvement is more than 20% and in case of JPEG compression, the improvement reaches more than 30%, especially when the image is compressed with high compression rate.

The convergence rate is other very important property for the Harris-Affine algorithm, in which final detected regions centered by the interest points are obtained after several iterations until the convergence criterion given by

$$\text{Conv - rate} = \frac{\#\ \text{of converged initial regions}}{\#\ \text{of initially detected regions}} \times 100 \quad (23)$$

is satisfied. If an interest region is obtained accurately in the initial step of the algorithm, this region can be converged after a few iterations, while if the initial estimation is not accurate, the interest region cannot satisfy convergence criterion even after considerably large iterations and finally this region may be discarded as interest region. Table 1 shows a comparison of the convergence rates of proposed Atomic Harris-Affine detector and the conventional Harris-Affine detector. Here the convergence rates are calculated by (21), using six images under different imaging conditions.

From Table 1, the convergence rates of the proposed detector are much better than that of the conventional one, providing more than 95% in all cases, and in case of the illumination variation, the convergence rate of the proposed detector is 30% better than that of the conventional one. This result means that the initial estimation of proposed detector is sufficiently accurate and then the algorithm can reach a convergence criterion after a few iterations, which is shown by Table 2.

Table 1. Comparison of convergence rates.

| | Point detection scheme | |
|---|---|---|
| Characteristics | Harris-Affine | Proposed |
| Blurring | 90.6% | 98.66% |
| Viewpoints | 91.83% | 99.30% |
| Scaling, rotation | 83.48% | 98.01% |
| Illumination | 65.56% | 95.33% |
| JPEG Compression | 91.54% | 99.66% |

Table 2. Average number of iterations required for each interest region until convergence

| | Point detection scheme | |
|---|---|---|
| Characteristics | Harris-Affine | Proposed |
| Blurring | 11.0 | 9.96 |
| Viewpoints | 9.40 | 6.82 |
| Scaling, rotation | 7.26 | 5.24 |
| Illumination | 11.25 | 5.64 |
| JPEG Compression | 8.26 | 6.31 |

From this table, the convergence time of the proposed detector is reduced from 20% to 50% compared with that of the conventional one, which is significant for many robot and other computer vision applications when a fast response is required.

# 4 Conclusion

In this paper a new Harris-Affine based interest point detector, denominated as Atomic Harris-Affine detector is proposed, in which the Gaussian kernel, that is used in the conventional detector, is replaced by the $up(x, y)$ 2D Atomic Function. The excellent properties, such as compact support and reduction of spectral leakage, of $up(x, y)$ function that is used as weighting function in scale and affine invariant detector were shown. The performance evaluations are carried out using several sequences of images with different imaging conditions, such as blurring level, illumination level, different viewpoints, different scaling factors and rotation angles, and compression rate by JPEG compression algorithm.

Evaluation results show that the proposed scheme can detect interest regions centered by interest points in more accurate manner than the conventional Harris-Affine detector, which is shown by repeatability rates and convergence rates of the interest regions. Evaluation results shows that the repeatability rate obtained by the proposed detector is about 14.7% higher than that obtained using the conventional detector, while the convergence rate is improved in about 14.6%. From these results, we can conclude that the proposed detector can be used in many computer vision applications in feasible manner. In addition to the better detection accuracy, the proposed detector provides a shorter response

time due to a fewer iterations required to reach a convergence criterion for each interest region, which is benefit to many applications where fast response is required.

*References:*


[1] L. Taehee, S. Stefano. Video-based descriptors for object recognition. *Image and Vision Computing* 2011, 29, 639–652.

[2] S. Dickinson, A. Leonardis, B. Schiele, M. Tarr Object recognition through reasoning about functionality: A survey of related works. In *Object Categorization: Computer and Human Vision Perspectives*, 1st ed.; Cambridge University Press, New York, USA, 2009; pp. 129-147.

[3] R. Szeliski Feature detection and matching. In *Computer Vision: Algorithms and Applications (Text in Computer Science)*, 1st ed.; Springer, New York, USA, 2011; pp. 181-227.

[4] H. Müller, P. Clough, T. Deselaers, B. Caputo, Object and concept recognition for image retrieval. In *Image CLEF: Experimental Evaluation in Visual Information Retrieval*, 1st ed.; Springer, London, UK, 2010; Volume 32, pp. 199-216.

[5] C. Harris, M. Stephens, A combined corner and edge detector, *In Proceedings of 4th Alvey Visual Conference*, Manchester, UK, 31st August – 2nd September 1988.

[6] K. Mikolajczyk, C. Schmid, Scale & affine invariant interest point detectors, *International Journal of Computer Vision* 2004, 60, 63–86.

[7] K. Mikolajczyk C. Schmid, An affine invariant interest point detector, In *Proceedings of 7th European Conference on Computer Vision*, Copenhagen, Denmark, 27th May – 2nd June 2002.

[8] S. Smith, J. Brady, SUSAN: A new approach to low level image processing. *International Journal of Computer Vision* 1997, 23, 45-78.

[9] D. Marr, Representing the image. In *Vision: A computational investigation into the human representation and processing of visual information*, W. H. Freeman, San Francisco, USA, 1982; pp. 54 - 78.

[10] T. Tuytelaars, K. Mikolajczyk, Local invariant feature detectors: A survey, *Foundations and Trends in Computer Graphics and Vision*, Now Publishers Inc. Hanover, USA, 2008; pp.3-64.

[11] P. Moravec, Obstacle avoidance and navigation in the real world by a seen robot rover, *Tech. report CMU-RI-TR-80-03, Robotics Institute, Carnegie Mellon University & doctoral dissertation*, Stanford University, Stanford, C.A, 1980.

[12] J. Shi, C. Tomasi, Good features to track. *In Proceedings of IEEE Conference on Computer Vision and Pattern Recognition*. Seattle, USA, 21-23 June 1994.

[13] P. Beaudet, Rotationally invariant image operators. In *Proceedings of the 4th International Joint Conference on Pattern Recognition*, Kyoto, Japan, 7-10 November 1978.

[14] R. Soumela, Robust image corner detection through curvature scale space, IEEE Transactions on pattern Analysis and Machine Intelligence, 1998, 20, 1376-1381.

[15] H. Bay, T. Tuytelaars, V. Gool, Surf: Speeded up robust features. *Journal of Computer Vision and Image Understanding*, 2008, 110, 346-359.

[16] D. Lowe, Distinctive image features from scale-invariant keypoints. *International Journal of Computer Vision*, 2004, 60, 91–110.

[17] C. Schmid, R. Mohr,C. Bauckhage, Evaluation of interest point detectors. *International Journal of Computer Vision*, 2000, 37, 151–172.

[18] K. Mikolajczyk, T. Tuytelaars, C. Schmid, A-Zisserman, J. Matas, F. Schaffalitzky, T. Kadir V. Gool, A comparison of affine region detectors. *International Journal of Computer Vision*, 2005, 65, 43–72.

[19] P. Moreels, P. Perona, Evaluation of features detectors and descriptors based on 3D objects. *International Journal of Computer Vision*, 2007, 73, 263–284.

[20] H. Aanæs A. Lindbjerg, K. Steenstrup, Interesting interest points: A comparative study of interest point performance on a unique data set. *International Journal of Computer Vision*, 2012, 97, 18-35.

[21] F. Yang, L. Wei, Z. Zhang, H. Tang, Image mosaic based on phase correlation and Harris operator. *Journal of Computational Information Systems*, 2012, 8, 2647–2655.

[22] W. Xiang, N. Pan, Y. Hong, C. Li, Affine invariant Image watermarking using intensity probability density-based Harris Laplace detector. *Journal of Visual Communications and Image Representation*, 2012, 23, 892–907.

[23] J. Zhang, L. Luo, Combined category visual vocabulary: A new approach to visual vocabulary construction. In *Proceedings of the 4th International Congress on Image and Signal Processing*, Shangai, China, 15-17 October 2011.

[24] F. Bellavia, M. Cipolla, D. Tegolo, C. Valenti An evolution of the non-parameter Harris Affine corner detector: a distributed approach. In *Proceedings of the International Conference on Parallel and Distributed Computing, Applications and Technologies*, Hiroshima, Japan, 8-11 December 2009.

[25] L. Sipiran, B. Bustos, Harris 3D: A robust extension of the Harris operator for interest point detection on 3D meshes. Journal of Vision Computing, 2011, 27, 963–976.

[26] M. Gevrekci K. Bahadir, Illumination robust interest point detection. *Journal of Computer vision and image understanding*, 2009, 113, 565–571.

[27] L, Zhang, I. Zhang, D. Zhang, A multi-scale bilateral structure tensor based corner detector. In *Proceedings of the 9th Asian Conference on Computer Vision*, Xi'an, China, 23-27 September 2009.

[28] V, Kravchenko, M. Basarab, V. Masyuk, R-functions, atomic functions and their applications. *Radioelektronika*, 2001, 8, 5-40.

[29] M. Cejudo-Torres, E. Garcia-Rios, E. Escamilla-Hernandez, M. Nakano-Miyatake, H, Perez-Meana, Counterfeit image detection on face recognition systems using stereo vision and optical flow methods, *WSEAS Modern Computer Applications on Science and Education*, 2014, pp. 40-45.

[30] M. Cejudo-Torres, E. Escamilla-Hernandez, M. Nakano-Miyatake, H. Perez-Meana, Improved optical flow estimation methods using atomic functions. In *Proceedings of Midwest Symp. on Circuits and System*, 2012.

[31] K. Perez-Daniel, E. Escamilla-Hernandez, M. Nakano-Miyatake, H. Perez-Meana, A novel image interest points detector based on Harris method using Atomic Functions, *Journal of Telecommunications and Radio Engineering*, 2012, pp. 1575-1588.

[32] K. Perez-Daniel, E. Escamilla-Hernandez, M. Nakano-Miyatake, H. Perez-Meana, An atomic function based approach of Harris-affine detector, Proc. Of SoMet, 2013, pp. 185-189,

[33] M. Brown, D. Lowe, Recognizing panoramas. In *Proceedings of the 9th International Conference on Computer Vision*, Nice, France, 13-16 October 2003

[34] M. Loog, F. Lauze, The improbability of Harris interest points. *IEEE Transactions on Pattern Analysis and Machine Intelligence*, 2010, 32, 1141–1147.

[35] T. Lindeberg, Feature detection with automatic scale selection. *International Journal of Computer Vision*, 1998, 30, 79-116.

[36] V. Kravchenko, Lectures on the Theory of Atomic Functions and their Applications, *Radiotekhnika*, 2003.

[37] Katholike Universiteit Leuven and INRIA Rhone-Alpes. Affine Covariant Features, Website, http://www.robots.ox.ac.uk/~vgg/research/affine/ Accessed on September, 2012.